



# Ca and Sr isotope constraints on the formation of the Marinoan cap dolostones

Guang-Yi Wei<sup>a,b,\*</sup>, Ashleigh v.S. Hood<sup>c</sup>, Xi Chen<sup>a</sup>, Da Li<sup>a</sup>, Wei Wei<sup>a</sup>, Bin Wen<sup>b</sup>, Zheng Gong<sup>b</sup>, Tao Yang<sup>a</sup>, Zhao-Feng Zhang<sup>d</sup>, Hong-Fei Ling<sup>a,\*</sup>

<sup>a</sup> State Key Laboratory for Mineral Deposits Research, Department of Earth Sciences, School of Earth Sciences and Engineering, Nanjing University, 163 Xianlin Avenue, Nanjing 210023, China

<sup>b</sup> Department of Geology and Geophysics, Yale University, New Haven, CT 06520, USA

<sup>c</sup> School of Earth Sciences, University of Melbourne, Parkville, VIC, 3010, Australia

<sup>d</sup> State Key Laboratory of Isotope Geochemistry, Guangzhou Institute of Geochemistry, the Chinese Academy of Sciences, Guangzhou 510640, China

## ARTICLE INFO

### Article history:

Received 29 July 2018

Received in revised form 9 January 2019

Accepted 12 January 2019

Available online 8 February 2019

Editor: D. Vance

### Keywords:

calcium isotope  
strontium isotope  
Marinoan cap dolostone  
meltwater  
mixing model  
deglaciation climate

## ABSTRACT

Neoproterozoic cap dolostones, which ubiquitously overlie Marinoan glacial diamictites, may record marine and climatic paleo-environmental conditions at the termination of the largest glacial epoch in Earth's history. Many geochemical indices have been used to interpret cap dolostone formation in the context of extreme climate change in the aftermath of the Marinoan glaciation. However, there are significant debates about whether these geochemical data represent global signals or regional sedimentary and/or diagenetic processes. Here we analyzed cap dolostones from three different continental cratons for their Ca-isotope, Sr-isotope and trace element compositions in order to obtain new insights into formation of the Marinoan cap dolostone and post-Marinoan paleo-environmental conditions (<~635 Ma). In three globally separated sections from South China (Yangtze Gorges area), North China (Northwest Tarim) and northwest Namibia, a similarly large negative  $\delta^{44}\text{Ca}$  excursion (~0.6‰), coupled to a positive  $^{87}\text{Sr}/^{86}\text{Sr}$  excursion, is recorded in the lower part of these cap dolostone successions. In the context of a relatively short duration for Marinoan cap dolostone (~10<sup>4</sup> year timescale), we propose that the preservation of both the large negative  $\delta^{44}\text{Ca}$  excursion and the positive  $^{87}\text{Sr}/^{86}\text{Sr}$  excursion in three widely-separated stratigraphic sections was not caused by globally uniform changes in isotopic compositions of the whole marine Ca and Sr reservoir. Instead, these excursions may have been caused by the addition of terrestrial meltwater and later deglacial runoff, carrying large amounts of Ca and Sr sourced from continental weathering into shallow seawater. A combined diagenetic-mixing model is used to track the coupled  $\delta^{44}\text{Ca}$  and  $^{87}\text{Sr}/^{86}\text{Sr}$  variations in the cap dolostones. Large inputs of terrestrial meltwater and deglacial runoff under high CO<sub>2</sub> atmospheric conditions in the aftermath of Marinoan glaciation is likely to have supplied abundant Ca, Mg and bicarbonate to shallow shelf seawater, helping facilitate cap dolostone deposition and contributing to the recorded negative Ca isotope excursion.

© 2019 Elsevier B.V. All rights reserved.

## 1. Introduction

The onset of the Ediacaran Period is characterized by widespread, thin cap dolostone successions which abruptly overlay the glacial diamictite and have been suggested to have formed under the warming of Earth's climate in the aftermath of the Marinoan 'Snowball Earth' glaciation (Hoffman et al., 1998, 2017). These

Marinoan cap dolostone units are characterized by buff-colored, micro-peloidal or microcrystalline dolomite, and show characteristic sedimentary structures including grading, ripples, teepee structures and sheet cracks (e.g., Jiang et al., 2003; Hoffman, 2011). Moreover, the cap dolostones generally preserve microbialite or stromatolite bioherms and/or 'tubestone' structures, barite and carbonate seafloor crystal fans (see Hoffman et al., 2017 for a review), and are overlain by dolomitic shale or carbonate (limestone or dolostone). Despite the variable stratigraphic thicknesses of cap carbonates in different sections (Hoffman et al., 2007), there is a consensus that cap dolostone deposition occurred during a major transgression in response to ice melting following the end of the Marinoan glaciation. However, the formation mechanism of

\* Corresponding authors at: State Key Laboratory for Mineral Deposits Research, Department of Earth Sciences, School of Earth Sciences and Engineering, Nanjing University, 163 Xianlin Avenue, Nanjing 210023, China.

E-mail addresses: wgyjnues@gmail.com (G.-Y. Wei), hfling@nju.edu.cn (H.-F. Ling).

the mysterious cap dolostone, which is ubiquitously distributed all over the world, is still debated. Based on stratigraphic, sedimentological and geochemical analyses of the cap dolostones, various hypotheses have been proposed for the formation of the cap dolostones, including: rapid deglaciation from a ‘Snowball Earth’ state (Hoffman et al., 1998; Higgins and Schrag, 2003), destabilization of methane hydrates (Jiang et al., 2003), a meltwater ‘plumeworld’ (Shields, 2005) or a condensed sequence from a multiphase transgression (Kennedy and Christie-Blick, 2011).

In addition to the debates on genesis of the Marinoan cap dolostone, there are also some doubts as to its timescale and temporal evolution. A short timeframe of several thousand years for cap dolostone formation was initially proposed based on the ‘Snowball Earth’ model (Hoffman et al., 1998; Higgins and Schrag, 2003). Conversely, much longer timescales of 0.1 Myr to 1 Myr have been suggested based on the preservation of multiple magnetic reversals (Font et al., 2010). Recent modeling or geochemical studies derived an intermediate timescale ( $\sim 10^4$  years) for cap dolostone deposition based on carbon cycle and energy models or the chemical composition of post-glacial barite fans (Ridgwell et al., 2003; Crockford et al., 2016; Yang et al., 2017). Moreover, there have been suggestions that the cap dolostone successions in marine basins are diachronous across different paleo-depths or within the sedimentary cross-section, with deep marine settings likely becoming ice-free and forming carbonate earlier than shelf settings (Hoffman et al., 2007; Rose and Maloof, 2010). Meanwhile, semi-diachronous conditions (i.e. diachronous basal cap dolostone and isochronous upper cap dolostone deposition) have been proposed by the plumeworld model, where a meltwater lens precipitated cap dolostones (Shields, 2005). Independent of these models, there is a correlation between the maximum thickness of a cap carbonate succession (sometimes including carbonate units stratigraphically above the cap dolostone) and its paleo-latitude, which could suggest longer durations of carbonate precipitation with earlier onset of ice melting in equatorial regions (Hoffman and Li, 2009) and a potential diachroneity for the basal cap dolostone.

Many stratigraphic and geochemical indices (e.g., C, Sr, Ca, S,  $\Delta^{17}\text{O}$  isotope systems) have been used to track the global environmental change in the aftermath of the Marinoan glaciation (e.g., Jiang et al., 2003; Yoshioka et al., 2003; Kasemann et al., 2014; Crockford et al., 2016). However, geochemical signatures of carbonates were likely susceptible to regional differences in sedimentary and diagenetic conditions across the global marine environment. The lack of systematic research on the behavior of various isotope systems during regional precipitation and diagenetic processes of the cap dolostone compromises the use of these indices to reconstruct the global deglacial atmospheric–oceanic environment. In order to better constrain the genesis of the Marinoan cap dolostone and associated environmental conditions, we studied the evolution of multiple geochemical indices (Ca and radiogenic Sr isotopes, trace element concentrations and ratios) for three widely separated sections, by considering the effects of sedimentary environment and early diagenesis on these proxies in the cap dolostone successions. Ca and radiogenic Sr isotopes of Marinoan cap dolostones from sections in South China, Northwest Namibia and Northwest Tarim consistently exhibit a co-varying trend in the lower cap dolostone successions, which can be well explained with a new diagenetic-mixing model. Based on this model, a novel scenario is proposed for cap dolostone formation, and the marine environment in the aftermath of the Marinoan glaciation.

## 2. Calcium isotopes as a paleo-environmental proxy

Calcium has a long residence time ( $\sim 0.5$ – $1$  million years (Myr)) and high concentration (10.3 mM) in the modern ocean (e.g., Fantle and Tipper, 2014). Over geological timescales (much longer

than 1 Myr), marine Ca isotopic variations (defined as  $\delta^{44}\text{Ca}$  for  $^{44}\text{Ca}/^{40}\text{Ca}$  ratios, relative to NIST SRM 915a in this study) are driven by variations in the Ca isotope compositions of its sources and sinks, specifically the oceanic carbonate sink (i.e. globally dominant precipitation of aragonite or calcite) (Fantle and Tipper, 2014). Riverine and hydrothermal inputs with relatively low  $\delta^{44}\text{Ca}$  values ( $\sim 0.9\text{‰}$ ) are the most important sources for the marine Ca reservoir. Marine carbonates are the most substantial sink for Ca, but different carbonate minerals have distinct fractionation factors for Ca isotopes relative to seawater. The fractionation for abiotic aragonite relative to seawater ( $\Delta_{\text{arag-sw}} = -1.6\text{‰}$  at  $25\text{ °C}$ ) is much larger than that for abiotic calcite ( $\Delta_{\text{cal-sw}} = -0.7$  to  $-1.1\text{‰}$ , where variation is controlled by precipitation rates) (see Gussone et al., 2016 for a review). Due to the preference for light Ca in the precipitated phase, the Ca isotopic composition of seawater is distinctively heavier than that of marine carbonate under steady-state conditions (a mean  $\delta^{44}\text{Ca}$  value of  $1.89\text{‰}$  for the modern ocean, Gussone et al., 2016). However, large increases in the Ca riverine input flux (with relatively low  $\delta^{44}\text{Ca}$  values) can perturb the marine Ca isotopic mass balance and result in negative marine Ca isotope excursions at  $\sim 1$  Myr timescales (e.g., Blättler et al., 2011). Numerical models (such as time-dependent Ca isotope mass balance model and reactive-transport model) predict changes in carbonate  $\delta^{44}\text{Ca}$  caused by: mineralogical transition (due to different Ca isotope fractionation between seawater and calcite or aragonite, Gussone et al., 2016); kinetics of precipitation (e.g., precipitation rate, Tang et al., 2008; Holmden et al., 2012a; Lau et al., 2017); early diagenesis (influence of pore fluids and/or meteoric fluids, e.g., Fantle and DePaolo, 2007; Ahm et al., 2018) or perturbations to the global Ca cycle over geological time frames (e.g., Payne et al., 2010; Blättler et al., 2011).

Based on research on modern and ancient carbonate sediments, the systematic relationship between Ca isotope and other proxies such as radiogenic Sr isotope, Sr concentration, Mg/Ca ratio in the carbonate, has been studied extensively to track the process of carbonate deposition and to reconstruct paleo-environmental conditions (e.g., Fantle and DePaolo, 2007; Blättler et al., 2011; Lau et al., 2017; Higgins et al., 2018). The Ca isotope system is particularly useful for studying Precambrian carbonate sequences because Ca is a major component of the carbonate crystal lattice and is therefore not easily affected by detrital contamination. Moreover, the combination of radiogenic Sr isotope analysis with Ca isotope data can provide additional insights into the climate and weathering evolution as well as dolostone formation mechanisms.

## 3. Geological setting

Marinoan cap dolostone samples ( $< \sim 635$  Ma) were collected from basal Ediacaran sequences from three geographically separated cratons. These localities include: 1) the Maieberg Formation (Keilberg Member (Mb.), in the Etoto section,  $17^{\circ}36'10.80''\text{S}$ ,  $14^{\circ}3'57.60''\text{E}$ ) from the Congo Craton, NW Namibia; 2) the Doushantuo Formation (Member I, the Jiulongwan section,  $30^{\circ}48'14.40''\text{N}$ ,  $110^{\circ}3'18.00''\text{E}$ ) from the Yangtze Craton, South China; 3) the Sugetbrak Formation (the Wushi section,  $40^{\circ}50'27.60''\text{N}$ ,  $79^{\circ}17'49.20''\text{E}$ ) from the Tarim Craton, North China (Fig. 1).

In the Etoto section of Namibia, the Keilberg Mb. cap dolostone is  $\sim 10$  m thick and composed of pinkish dolomite, gradationally overlain by silty, finely laminated limestone (Fig. 1). In this locality, the Keilberg Mb. was likely to have been deposited on the upper slope of the Otavi carbonate platform, below or near wave base (Hoffman et al., 2007). The Doushantuo Formation of the Jiulongwan section in the Yangtze Three Gorges area represents a shallow marine environment, in an inner shelf lagoon (Jiang et

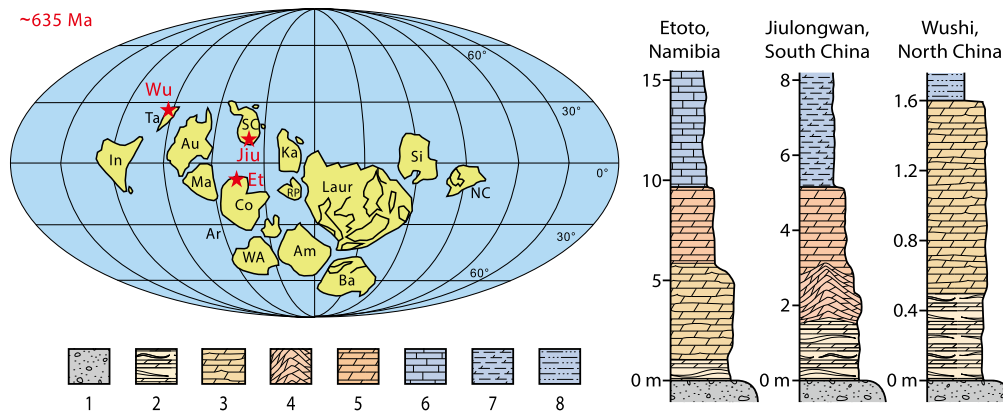


**Fig. 1.** Global paleogeography in the aftermath of the Marinoan glaciation at ~635 Ma (modified from Li et al., 2008). The sections studied for cap carbonates are (Et) Etoto section, Northwest Namibia (Hoffman, 2011); (Jiu) Jiulongwan section, South China (Jiang et al., 2003); and (Wu) Wushi section, Northwest Tarim (Wen et al., 2015). Lithological patterns: 1 – diamictite, 2 – disrupted dolostone with sheet-crack cements, 3 – laminated dolostone with tepee-like structures, 4 – dolostone with low-angle cross-bedding/incipient tepee development, 5 – laminated dolomite, 6 – laminated limestone, 7 – dolostone interbedded with black shale, 8 – siltstone. (For interpretation of the colors in the figure(s), the reader is referred to the web version of this article.)

al., 2003). At the base of the Doushantuo Formation, the 5-m-thick cap dolostone unit overlies the Nantuo glacial diamictites (Fig. 1). The upper cap dolostone unit contains a volcanic ash layer which has been dated at  $635.2 \pm 0.6$  Ma with zircon U–Pb methods (Condon et al., 2005). The cap dolostone consists of finely-crystalline dolostone and laminated silty subordinate limestone or dolostone, which were probably deposited during the later stages of deglacial transgression, and likely deposited below or near wave base (Ling et al., 2013). In the Wushi section of the northwestern Tarim craton, the cap dolostone is ~1.0–1.7 m thick and composed of pink, thin-laminated, finely-crystalline dolostone, similar to many other Marinoan cap dolostones (Wen et al., 2015).

#### 4. Materials and methods

Carbonate samples were carefully selected to avoid non-carbonate detritus and late-stage veining and/or alteration, and powders were drilled from well-preserved rock pieces. For major/trace element and Ca isotope analyses of bulk carbonate samples, approximately 50 mg of each sample was weighed and then leached with 0.1 M hydrochloric acid (HCl) to dissolve and extract the carbonate fraction. Major and trace elements in the leachates were measured with a Thermo Element-II inductively-coupled plasma mass spectrometer (ICP-MS) at Nanjing University and Thermo Element-XR ICP-MS at Yale University, and relative standard deviations were better than 5%.

For Ca-isotope analyses, a two-step resin column method was used for Ca separation, and Ca isotope was analyzed with Thermo Neptune Plus multi collector (MC)-ICP-MS with a ESI Apex-IR desolvating system at Yale Metal Geochemistry Center (YMGC). All samples were bracketed by NIST-SRM-915a standard (processed through columns to remove Sr) to calibrate the fractionation during analysis. Measured  $^{44}\text{Ca}/^{42}\text{Ca}$  values are presented in delta notation,  $\delta^{44/42}\text{Ca}$ :

$$\delta^{44/42}\text{Ca} = \left[ \left( \frac{^{44}\text{Ca}/^{42}\text{Ca}}{\text{sample}} / \left( \frac{^{44}\text{Ca}/^{42}\text{Ca}}{\text{NIST-SRM-915a}} \right) - 1 \right) * 1000 \right]$$

Measurement uncertainty for each sample is  $\pm 0.03\text{‰}$  (2SE) and the long-term external reproducibility of Ca isotope analyses is better than  $0.075\text{‰}$  (2SD) for  $\delta^{44/42}\text{Ca}$  (OISL seawater standard:  $\delta^{44/42}\text{Ca} = 0.94\text{‰} \pm 0.075\text{‰}$  ( $n = 40$ , 2SD)). All the Ca isotope data have been converted to  $\delta^{44}\text{Ca}$  ( $^{44}\text{Ca}/^{40}\text{Ca}$ ) notation for comparison with other published data, using a kinetic fractionation law:  $\delta^{44}\text{Ca}$

$= \delta^{44/42}\text{Ca} * 2.09$  (Holmden et al., 2012b). More detailed methods and standard measurements of Ca isotopes are given in the supplementary materials.

For Sr-isotope analyses, carbonate leaching and Sr separation procedures followed those of Li et al. (2011). Sr isotope values were determined using a Triton MC-TIMS at Nanjing University and a Neptune Plus MC-ICP-MS at YMGC, Yale University. Repeated measurement of the Sr standard NIST SRM 987 yielded  $^{87}\text{Sr}/^{86}\text{Sr} = 0.710252 (\pm 0.000016)$ .

C and O isotopes of the carbonate samples were analyzed with a Thermo Kiel IV online carbonate preparation device + MAT 253 mass spectrometer at the Yale Analytical and Stable Isotope Center (YASIC) and a Finnigan Gasbench II online analysis system + Delta Plus XP at the State Key Laboratory for Mineral Deposits Research, Nanjing University. The results of C–O isotope are reported relative to V-PDB, and external analytical precision for C and O isotopes is  $0.06\text{‰}$  (2SD) and  $0.07\text{‰}$  (2SD), respectively, based on the replicate analyses of in-house (PX, TS) and international (NBS19) standards at YASIC, and the Chinese GBW00405 carbonate standard at Nanjing University.

#### 5. Results

Significant systematic variability in  $\delta^{44}\text{Ca}$ ,  $\delta^{13}\text{C}$ ,  $\delta^{18}\text{O}$ ,  $^{87}\text{Sr}/^{86}\text{Sr}$  ratios and some trace metal concentrations was recorded in each of the three cap dolostone sections (Table S1; Figs. 2 and 3). Trends in each of Ca, C, O and Sr isotopes up-section are broadly similar among the three sections. Aluminum, thorium concentrations and Rb/Sr ratios of all samples in the three sections are lower than 0.2%, 0.6 ppm and 0.01, respectively.

In the Etoto section, the lower three meters of the 10 m-thick cap dolostone show co-varying negative excursions in C and O isotopes ( $\delta^{13}\text{C}$  from  $-1.2\text{‰}$  to  $-3.6\text{‰}$ ;  $\delta^{18}\text{O}$  from  $-5.0\text{‰}$  to  $-8.8\text{‰}$ ) (Fig. 2). Ca isotopes also show a significant negative excursion over the lower three meters (from  $1.38\text{‰}$  to  $0.7\text{‰}$ ). Upward in the section,  $\delta^{44}\text{Ca}$  values return to  $1.42\text{‰}$  while  $\delta^{13}\text{C}$  and  $\delta^{18}\text{O}$  values remain relatively constant ( $\sim -3.3\text{‰}$  and  $-8.5\text{‰}$ , respectively).  $^{87}\text{Sr}/^{86}\text{Sr}$  ratios show a positive excursion (from 0.7087 to 0.7122) in the lower part of the cap dolostone, roughly correlated with the negative excursion in  $\delta^{44}\text{Ca}$ . There is no significant variation in Mg/Ca ratios or Sr concentrations up-section (Fig. 3). Limestones (from 10 m to 15 m in this section) overlying the cap dolostones show less negative  $\delta^{13}\text{C}$  and  $\delta^{18}\text{O}$  values ( $\sim -2.2\text{‰}$  and  $-6.0\text{‰}$ , respectively); relatively low Mg/Ca ratios ( $\sim 0.04$ ); low  $^{87}\text{Sr}/^{86}\text{Sr}$  (from 0.7074 to 0.7082); and high  $\delta^{44}\text{Ca}$  (from  $1.35\text{‰}$  to  $1.49\text{‰}$ ).

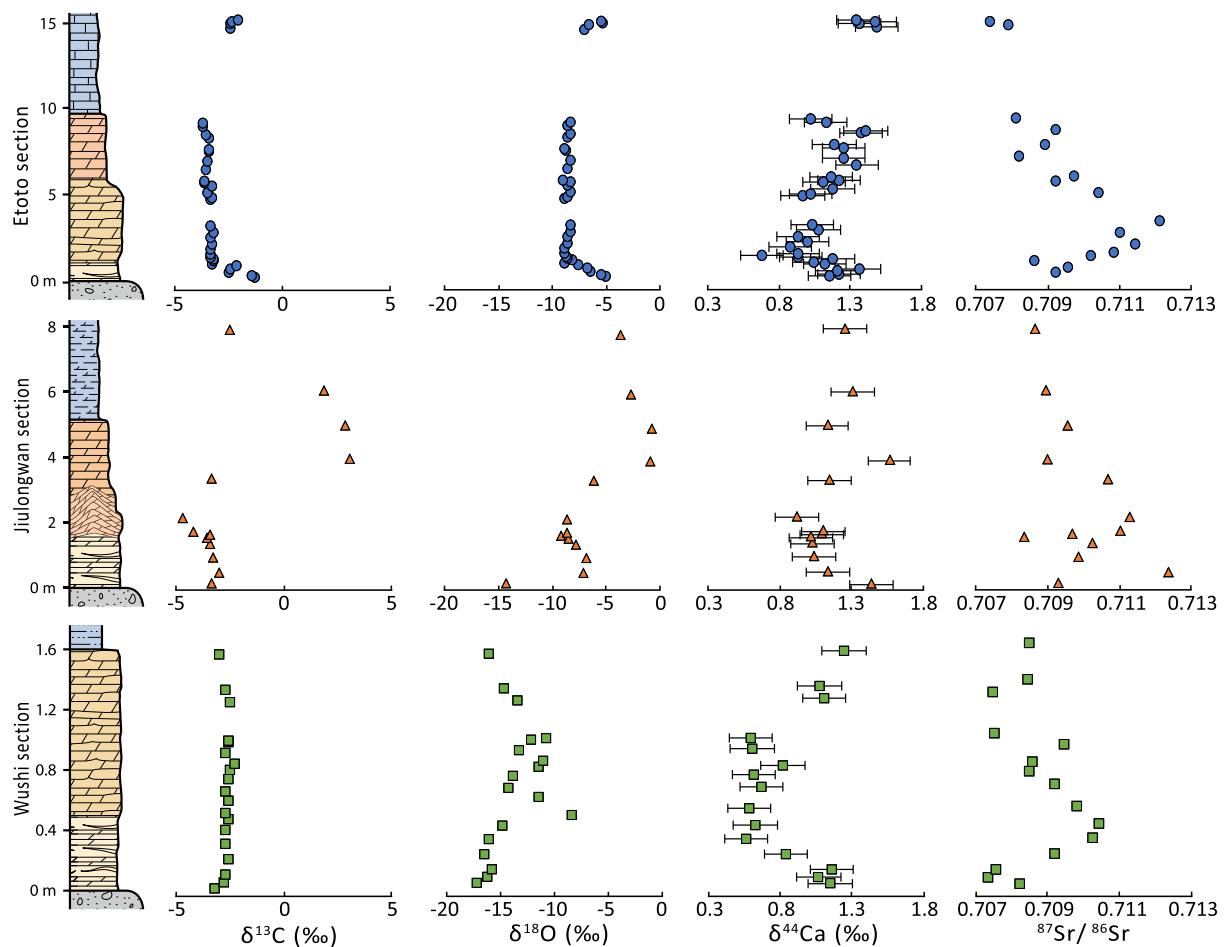


**Fig. 2.** Carbon, oxygen, calcium and strontium isotopic compositions of the carbonates in Etoto section (upper), NW Namibia, Jiulongwan section (middle), South China and Wushi section (lower), NW Tarim. Error bar for Ca isotopes is  $\pm 0.15$  (2SD), which is the long-term reproducibility of Ca isotope analyses.

In the Jiulongwan section, a significant negative Ca isotopic excursion (from 1.44‰ to 0.92‰) is observed with negative  $\delta^{13}\text{C}$  values (from  $-3.0$ ‰ to  $-4.7$ ‰) and  $\delta^{18}\text{O}$  values (from  $-6.1$ ‰ to  $-13.8$ ‰) in the lower part of cap dolostone (0–3 m) (Fig. 2). From 3 to 8 m,  $\delta^{13}\text{C}$  and  $\delta^{18}\text{O}$  values are relatively high (from  $-2.9$ ‰ to 3.1‰ and from  $-0.2$ ‰ to  $-3.3$ ‰, respectively) and  $\delta^{44}\text{Ca}$  values return to relatively high values (from 1.13‰ to 1.56‰).  $^{87}\text{Sr}/^{86}\text{Sr}$  ratios vary throughout the section (from 0.7084 to 0.7123) with a peak value of 0.7123 in the lowest meter of the cap dolostone, but with some scatter. There is no significant variation in Mg/Ca ratios or Sr concentrations of the studied samples (Fig. 3).

Similar  $\delta^{44}\text{Ca}$  and  $^{87}\text{Sr}/^{86}\text{Sr}$  variations to the Jiulongwan section are observed in the Wushi section, with a large negative Ca isotopic excursion (from 1.17‰ to 0.58‰) and relatively high  $^{87}\text{Sr}/^{86}\text{Sr}$  ratios (up to 0.7105) in the lower several meters of the cap dolostone (Fig. 2).  $\delta^{13}\text{C}$  values of the Wushi section samples are around  $-2.5$ ‰ with little variation, while the  $\delta^{18}\text{O}$  values vary significantly (beginning with extremely low values  $-17.3$ ‰, rising to  $-8.5$ ‰ in the middle, and ending with  $-16.1$ ‰ at the top). Similarly, there is no systematic variation in Mg/Ca ratios or Sr concentrations (Fig. 3).

## 6. Discussion

### 6.1. Possible effects of detrital contamination and late stage diagenesis on the cap dolostones

To constrain the processes that give rise to the consistent Ca–Sr isotope excursions across multiple, geographically-separated, sec-

tions of the Marinoan cap dolostones, it is important to consider the effects of depositional and diagenetic processes on their Ca and Sr isotope compositions, as well as to assess potential contamination from non-carbonate inclusions.

The incorporation of terrigenous silicate detritus in geochemical sampling may impact the measured geochemical signals in marine carbonates. Due to their extremely low concentrations in seawater and pure marine carbonates, Al and Th are generally used to investigate the influence of a detrital silicate component on marine carbonate geochemistry. Rb/Sr ratios can also be used to test the preservation of primary  $^{87}\text{Sr}/^{86}\text{Sr}$  signals in marine carbonates as terrigenous detritus (e.g., clay) has high Rb relative to Sr (cf. Sawaki et al., 2010; Ling et al., 2013; Zhao and Zheng, 2017; Wei et al., 2018). Samples in this study show relatively low Al and Th concentrations ([Al] < 0.6%, [Th] < 0.6 ppm) and Rb/Sr ratios (< 0.01) and no systematic correlation of  $\delta^{44}\text{Ca}$  or  $^{87}\text{Sr}/^{86}\text{Sr}$  vs. Al or Th concentrations or Rb/Sr ratios (Fig. S6), which suggests no significant detrital or Rb-decay impacts on isotopic signals in the studied carbonate samples.

Previous studies have considered the high Mn/Sr and  $^{87}\text{Sr}/^{86}\text{Sr}$  ratios of the cap dolostones in South China as a result of late stage diagenetic alteration (e.g., Sawaki et al., 2010; Bristow et al., 2011). However, the Precambrian ocean may have had high Mn concentrations owing to the dominantly anoxic or hypoxic seawater. In this sense, high Mn/Sr ratios in cap dolostones may not necessarily indicate the influence of late stage alteration, but may have simply reflected dominantly low  $\text{O}_2$  concentrations in the seawater or pore water. Further, the extreme  $^{13}\text{C}$ -depleted signatures ( $\delta^{13}\text{C}$  as low as  $-48$ ‰) with high Mn/Sr and  $^{87}\text{Sr}/^{86}\text{Sr}$  ratios reported

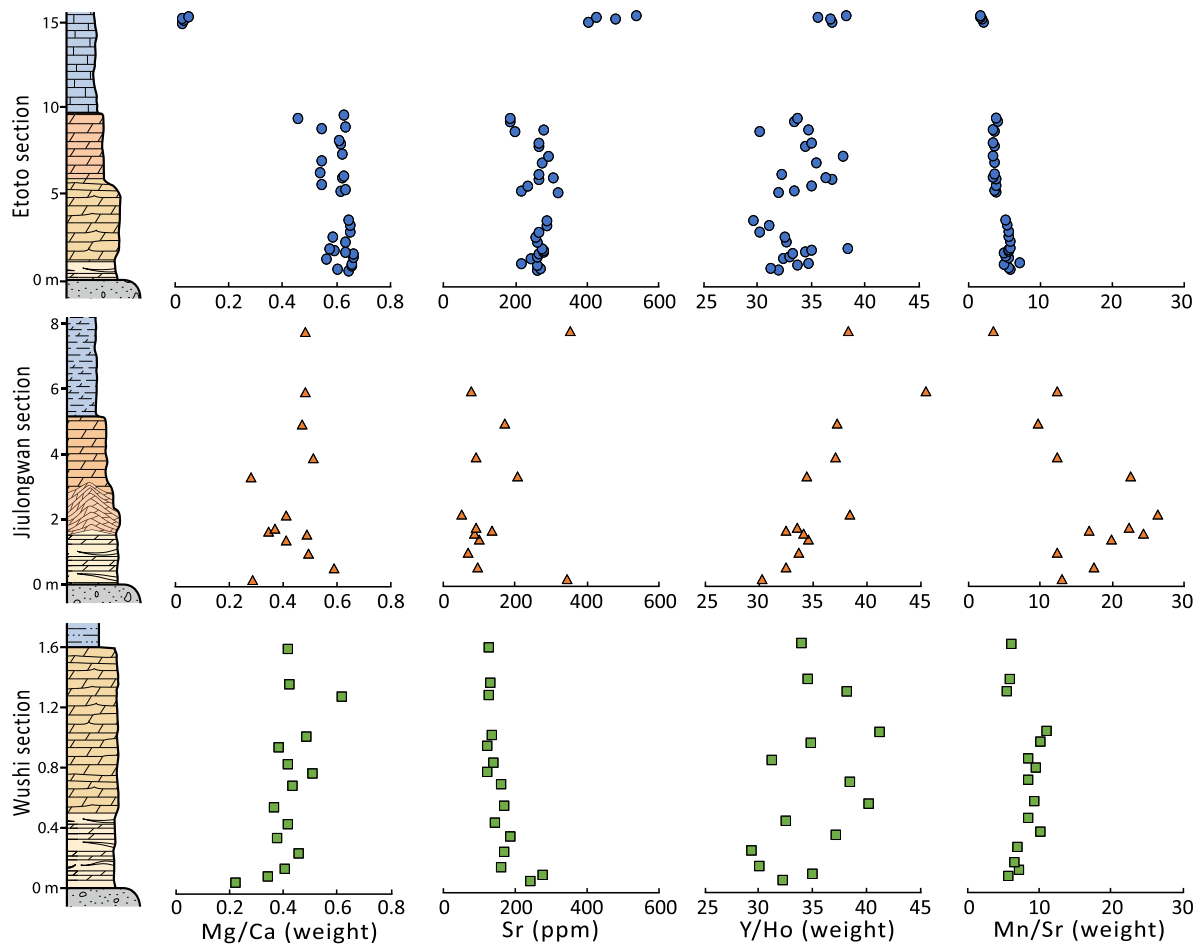


**Fig. 3.** Mg/Ca ratios, Sr concentrations, Y/Ho ratios and Mn/Sr ratios for carbonates in the Etoto section, NW Namibia, the Jiulongwan section, South China and the Wushi section, NW Tarim.

in the previous study, are measured from late-stage calcite veins in South China (Bristow et al., 2011). Neither calcite filled veins nor diagenetic barites were found in the cap dolostone successions from Namibia or North China discussed here (Hoffman, 2011; Wen et al., 2015). And relatively high  $^{87}\text{Sr}/^{86}\text{Sr}$  ratios as well as high Mn/Sr ratios are also observed in other cap dolostones from Namibia, Australia and Mongolia (Yoshioka et al., 2003; Liu et al., 2014), which are not considered to be a result of late-stage alteration. Hence, it cannot be simply concluded that high Mn/Sr ratios in the dolomitic matrix, without evident late-stage structures, are caused by late-stage alteration. Carbonate deposition and early diagenesis in anoxic or hypoxic seawater could also result in high Mn/Sr or  $^{87}\text{Sr}/^{86}\text{Sr}$  ratios in Precambrian dolostones (e.g., Banner, 1995; Hood and Wallace, 2015).

## 6.2. A 'global' Ca isotope record in the Marinoan cap dolostones?

In previous studies, Ca isotopes have been used to track changes in global continental weathering fluxes over geological time frames owing to the long oceanic residence time of calcium. Based on global time-dependent mass balance models, some negative Ca isotopic excursions in the Phanerozoic record (e.g., Permian-Triassic boundary; Cretaceous Ocean Anoxic Events) have been suggested to be driven by high continental weathering fluxes and/or ocean acidification in response to high atmospheric  $\text{CO}_2$  or large igneous provinces (LIPs) (e.g., Payne et al., 2010; Blättler et al., 2011). Previous studies on Neoproterozoic carbonates showed large negative Ca isotopic excursions in the laminated limestones overlying the cap dolostones in Brazil, Namibia and Canada (Fig. 4),

which have been interpreted as a result of extremely intense global chemical weathering in the aftermath of the Marinoan glaciation (Silva-Tamayo et al., 2010; Kasemann et al., 2014). However, these Ca isotope excursions are not the same as those observed in the cap dolostone successions in this study, and would not reflect the sedimentary environment at the onset of deglaciation. Moreover, crystal fans interpreted as formerly aragonite (from their pseudohexagonal prismatic habit) are interbedded in these limestone successions overlying the cap dolostones (e.g., Hoffman, 2011), and Sr concentrations of these limestones are significantly higher than expected in either calcite or dolostone (e.g., Yoshioka et al., 2003; Sial et al., 2010). Thus, besides the potential effect of continental weathering flux variations on marine Ca isotopes, there may have been mineralogical controls (cf. Jost et al., 2017), which variably exaggerated the negative Ca isotopic excursions preserved in the limestones in various sections (even up to 1.5‰), depending on the amount of aragonite precipitation (Fig. 4). Therefore, although extremely high weathering input of Ca into the ocean might in principle have induced a negative Ca isotope excursion in the cap dolostones, the effects of other factors such as regional diagenetic alteration and mineralogical transitions on Ca isotope during ancient carbonate deposition need to be examined (cf. Holmden et al., 2012a; Jost et al., 2017; Higgins et al., 2018) (discussed in section 6.3).

The tightly co-varying Ca and Sr isotopes from the three separated sections in this study are inconsistent with the global marine Ca and Sr geochemical cycles as the positive Sr isotope excursion would take a longer time for recovery than the negative Ca isotope excursion, due to the significantly longer residence time of Sr

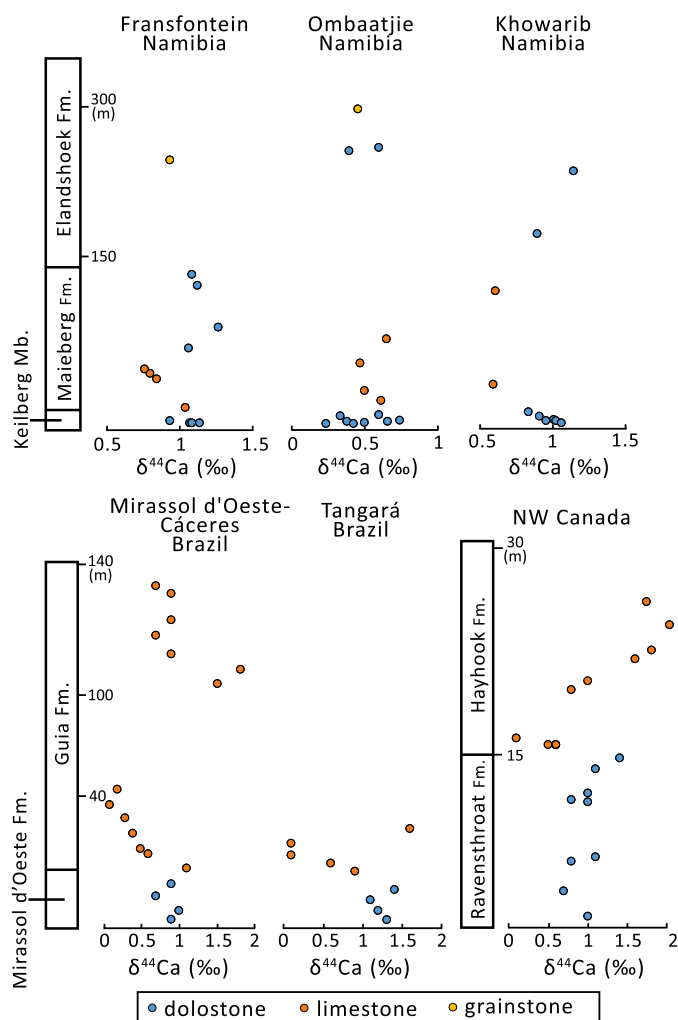


**Fig. 4.** Ca isotopic variations in the lower Ediacaran carbonate successions from Namibia, Brazil and Canada (data from Silva-Tamayo et al., 2010; Kasemann et al., 2014).

in the ocean, relative to Ca (cf. Holmden et al., 2012a). Considering the diachroneity in cap dolostone deposition (Hoffman et al., 2007) and a significantly longer time scale ( $\sim 10^4$  years) for deglacial ocean mixing (Yang et al., 2017), it is unlikely that the co-varying Ca and Sr isotope excursions observed in sections from different regions solely reflect a contemporaneous response to global fluctuation in the oceanic Ca and Sr isotope systems due to a very short period of intense deglacial continental weathering. Further, it is noteworthy that the three cap dolostone successions in this study do not show the same absolute  $\delta^{44}\text{Ca}$  and  $^{87}\text{Sr}/^{86}\text{Sr}$  values, despite a similar magnitude of  $\delta^{44}\text{Ca}$  excursion ( $\sim 0.6\text{‰}$ ). Taken together, these observations suggest that while a common process caused the Ca and Sr isotope anomalies, this process would be dominantly controlled by regional sedimentary environment and early diagenesis, rather than a fluctuation in the global oceanic reservoirs of Ca and Sr.

### 6.3. The impacts of regional sedimentary environment and early diagenesis on Ca and Sr isotopes in the cap dolostones

Studies of modern marine sediments indicate that early diagenesis affect the geochemical compositions of marine carbonates. Thus variations in different isotopes in the sediments can be driven by changes in diagenetic conditions (e.g., Fantle and DePaolo, 2007; Higgins et al., 2018). Based on research on modern Bahamian car-

bonates, the transition in early diagenetic conditions (i.e. from a fluid-buffered condition to a sediment-buffered condition) could induce significant Ca isotope variations in the sedimentary column (Higgins et al., 2018; Ahm et al., 2018). Shallow carbonate sediments and pore water near the sediment–water interface are proximal to the diagenetic fluid source and buffered by the geochemical signal of the fluid (fluid-buffer condition), whereas progressive interaction between pore fluid and carbonate sediments at depth within a sedimentary column potentially drives the pore fluid towards a geochemical signal approaching the sediment (sediment-buffered condition) (Ahm et al., 2018). As the Neoproterozoic oceans were dominated by aragonite precipitation (Hood and Wallace, 2018; Pruss et al., 2018), it is likely that cap dolostones were formed by early diagenetic dolomitization of aragonitic precipitates. In recent and modern carbonates, aragonite generally shows lower  $\delta^{44}\text{Ca}$  values ( $\sim 0.3\text{‰}$ ) and higher Sr ( $\sim 7000$  ppm) concentrations compared to calcite (about  $0.8\text{‰}$ – $1.0\text{‰}$  of  $\delta^{44}\text{Ca}$ , less than 900 ppm of Sr) (e.g., Banner, 1995; Higgins et al., 2018). Sr concentrations in dolomites may vary with the type of dolomitizing fluid (marine pore water or mixing meteoric–marine fluids) (Banner, 1995), whereas  $\delta^{44}\text{Ca}$  values of modern dolomites are distinctly higher than those of their precursors, aragonite and calcite (Higgins et al., 2018). In addition,  $\delta^{44}\text{Ca}$  values and Sr concentrations in bulk carbonates can also be affected by precipitation rates (Tang et al., 2008). Thus, examination of the relationship among multiple geochemical indices from the finely-crystalline dolomite matrix of cap dolostones (e.g. correlation or co-variation in Mg/Ca,  $\delta^{44}\text{Ca}$ , Sr concentration and  $^{87}\text{Sr}/^{86}\text{Sr}$ ) may help determine the sedimentary and early diagenetic processes for the Marinoan cap dolostone (cf. Lau et al., 2017; Higgins et al., 2018; Ahm et al., 2018).

With these considerations, we apply a recently developed early marine diagenetic model (modified after Ahm et al., 2018) to describe the variation in Mg/Ca ratios,  $\delta^{44}\text{Ca}$  values, Sr concentrations, and  $^{87}\text{Sr}/^{86}\text{Sr}$  ratios during the formation of cap dolostones. This model can be used to test deglacial shelf seawater as the dolomitizing fluid and to determine if changes in diagenetic conditions could have caused the coupled Ca–Sr isotope excursions in the Marinoan cap dolostones. Modeling processes are presented as changes in geochemical tracers with the increasing cumulative mass of fluid, interacting with the initial carbonate mineral under the fluid-buffered condition (box 1 in Fig. S3) and sediment-buffered condition (box N in Fig. S3) (model parameters are in the supplementary materials, see Table S3). The correlation of different geochemical indices derived from this diagenetic model (Fig. S3) are compared with the measured data from the cap dolostones in Fig. 5, and discussed below in relation to recent marine carbonate records. For Phanerozoic carbonates, one way of tracking the diagenetic conditions during dolomitization is to compare  $\delta^{44}\text{Ca}$  values and Sr concentrations (Ahm et al., 2018). Dolostones formed through sediment-buffered dolomitization of initial high-Mg calcite or aragonite might produce relatively low  $\delta^{44}\text{Ca}$  values, but show inherited high Sr concentrations. In contrast, dolostones formed through fluid-buffered dolomitization would yield high  $\delta^{44}\text{Ca}$  and low Sr concentrations (Ahm et al., 2018). Modern carbonate platforms can show excursions in  $\delta^{44}\text{Ca}$  due to the change between the two diagenetic conditions over several hundred meters depth within sediments (Higgins et al., 2018; Ahm et al., 2018). However, compared with the several hundred-meter deep scale of fluid interaction in modern carbonate platforms, the relatively thin cap dolostone succession could have been dolomitized more extensively in shelf seawater simply due to their lesser volume. The complete extent of dolomite cementation of micro-peloidal lithologies in early diagenesis (as evidenced by the syngedimentary formation of sheet cavities and teepee structures) also suggests high permeability in the original lithology and in-

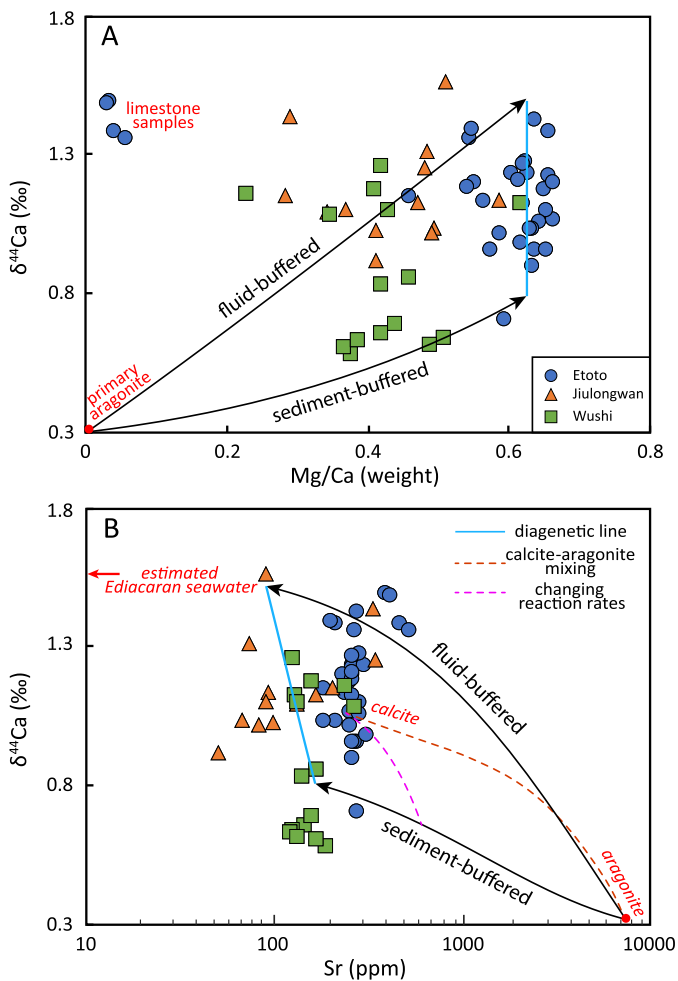


**Fig. 5.** Cross-plots of  $\delta^{44}\text{Ca}$  values vs. Mg/Ca ratios (A) and Sr concentrations (B) for the cap dolostone samples in this study compared to modeled values. Black arrows are the modeled curves for early marine dolomitization under fluid-buffered and sediment-buffered conditions (modified from Ahm et al., 2018). Blue lines show changes in geochemical signals for the diagenetic minerals under different diagenetic conditions. Purple and red dashed lines in (B) show the results of calcite-aragonite mixing and correlation of  $\delta^{44}\text{Ca}$  values and Sr concentrations controlled by various carbonate precipitation rates (Tang et al., 2008), respectively. Model parameters are given in the supplementary materials Table S3.

teraction with a large volume of fluid. Moreover, all of the cap dolostone samples in this study (except for the interval of the negative excursion) show high  $\delta^{44}\text{Ca}$  values with distinctly high Mg/Ca ratios and low Sr concentrations (Figs. 2 and 3). All of these observations suggest that the dolostones were formed through intensive fluid-buffered dolomitization of aragonite. Modeling results, combined with geochemical data in this study, indicate that the variations of  $\delta^{44}\text{Ca}$ , Mg/Ca, Sr concentration and  $^{87}\text{Sr}/^{86}\text{Sr}$  in the cap dolostones do not replicate the modeled trajectories expected from the transitions between the two different marine diagenetic conditions (Figs. 5 and Fig. 6A). Therefore,  $\delta^{44}\text{Ca}$  and  $^{87}\text{Sr}/^{86}\text{Sr}$  excursions over several meters of stratigraphy in the cap dolostones are very unlikely to have been caused by variations between fluid-buffered and sediment-buffered diagenetic conditions. Additionally, the lack of clear correlations between  $\delta^{44}\text{Ca}$  and Sr concentrations, or any petrographic evidence for the presence of variable calcite or aragonite precursor mineralogies, indicates no significant impacts derived from mineralogical variation or kinetic effects (Fig. 5B) (cf. Lau et al., 2017).

Although the formation mechanism for the Marinoan cap dolostones continues to be debated, it is generally thought to be related to marine transgression and a warming climate accompa-

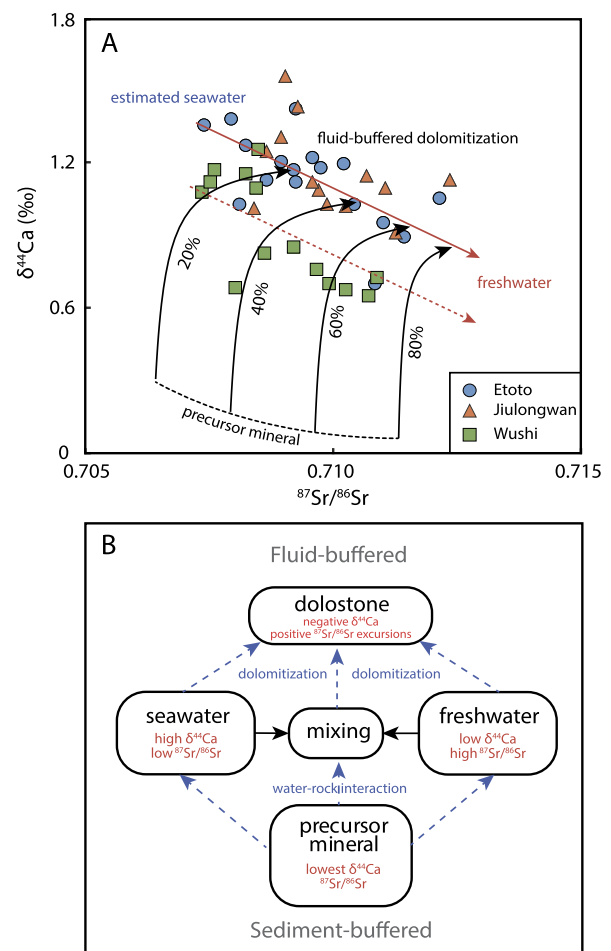


**Fig. 6.** (A) Modeling results for coupled variations of  $\delta^{44}\text{Ca}$  and  $^{87}\text{Sr}/^{86}\text{Sr}$  in Marinoan cap dolostones. The isotopic composition of the dolostone after the synsedimentary dolomitization in the mixed freshwater-seawater is calculated as below:  $\delta_{\text{mix}} = \delta_{\text{freshwater}} \times f + \delta_{\text{seawater}} \times (1 - f) + \Delta_{\text{recry}}$  where  $f$  is the proportion of total Ca or Sr amounts derived from freshwater and  $\Delta_{\text{recry}}$  is the isotopic fractionation between recrystallized mineral and the fluid (see supplementary materials Table S3 for modeling parameters). Red solid arrow represents a mixture between a meltwater fluid ( $\delta^{44}\text{Ca} = 0.89\text{‰}$  and  $^{87}\text{Sr}/^{86}\text{Sr} = 0.7150$ , Gussone et al., 2016; Blum and Erel, 1995) and a seawater ( $\delta^{44}\text{Ca} = 1.5\text{‰}$ ;  $^{87}\text{Sr}/^{86}\text{Sr} = 0.7070$ , estimated from the results of the studied samples and Cryogenian background values). Red dashed arrow is a mixing line with large Ca isotope fractionation during the recrystallization. Black arrows are modeled changes in  $\delta^{44}\text{Ca}$  and  $^{87}\text{Sr}/^{86}\text{Sr}$  during fluid-buffered synsedimentary dolomitization (Box 1 mode in the early marine diagenetic model in Fig. S3) under different fluid conditions (increased meltwater proportions). Black dashed curve represents the isotopic compositions of an aragonitic precursor (low  $\delta^{44}\text{Ca}$  and  $^{87}\text{Sr}/^{86}\text{Sr}$ ). (B) Schematic diagram showing synsedimentary dolomitization for the Marinoan cap dolostone formations under different fluid conditions.

nying the Marinoan deglaciation. Hoffman et al. (1998) suggested that cap dolostones were rapidly deposited during or immediately following the abrupt termination of a ‘Snowball Earth’, characterized by the laminated accumulation of micro-peloidal dolomite grains and dolomitic matrix, and teepee-like structures and/or cemented sheet cracks (e.g., Hoffman, 2011). Considering that cap dolostones are commonly overlain by (non-dolomitized) limestone, the dolomitization of the rapidly formed cap dolostone in such a short period is likely to have been synsedimentary or very early diagenetic; in other words, the dolomitization occurred in continental shelf seawater immediately following the primary aragonite succession (e.g., Font et al., 2006; Hood and Wallace, 2012, 2018; Pruss et al., 2018). The synsedimentary dolomitization of aragonitic precursor for the cap dolostone in this study is supported by high

Ba concentrations and low Cu concentrations of the dolostone samples (Fig. S7, e.g. dolomitized aragonite) which are also observed in other Neoproterozoic synsedimentary dolostones formed in a shallow marine environment (Hood and Wallace, 2012, 2015). Several mechanisms/factors may have promoted synsedimentary dolomitization in Precambrian marine environments, including low oxygen and high-Mg global seawater conditions favoring microbially-mediated dolomite formation on a broad scale (e.g. Burns et al., 2000; Gammon, 2012; Hood and Wallace, 2012). Additionally, sulfate-reducing bacteria could directly mediate the precipitation of primary dolomite, which generally preserve microbial fabrics, spherulitic crystal forms and have relatively high Sr concentrations (3000–6000 ppm) (e.g., Sánchez-Román et al., 2011). However, the Marinoan cap dolostones are depleted in Sr (Fig. 3), extensively cemented by dolomite and lack abundant microbialites (except for stromatolite bioherms overlying the basal cap dolostone). Thus, we suggest that the cap dolostone was formed through immediate dolomitization of primarily precipitated aragonite (i.e. synsedimentary dolomitization) in shelf shallow water under anoxic marine conditions favorable to microbial activity, but not necessarily through directly microbially-mediated dolomite precipitation (e.g., Burns et al., 2000; Font et al., 2006; Hood and Wallace, 2012; Gammon, 2012; Fabre et al., 2013).

In conclusion, the Marinoan cap dolostones are suggested to be formed by accumulation of dolomite layers that were transformed from primarily precipitated aragonite through synsedimentary dolomitization under a continuous fluid-buffered condition. Although the recrystallization of primary carbonate minerals and fluid flow rates are poorly constrained for Marinoan cap dolostones, the rate of early diagenesis or dolomitization in the shallow carbonates can be fast (Land, 1973; Swart et al., 1987). The rate of synsedimentary dolomitization for the Marinoan cap dolostone successions may have been faster than that of Cenozoic carbonates due to inferred high Mg/Ca throughout the Neoproterozoic (Hood and Wallace, 2018) as well as thermal imbalances and a large amount of hydraulic head pumping fluid across shelves during deglaciation. As a result, the isotopic signals of the primary aragonite were overprinted by the dolomitizing fluid, whose composition was evolving during the deglaciation process. Thus, geochemical signatures of each dolomite layer of the whole cap dolostone succession would reflect instantaneous fluid–mineral interaction, which changed with evolution of the shelf seawater. In light of this, the variations of  $\delta^{44}\text{Ca}$  and  $^{87}\text{Sr}/^{86}\text{Sr}$  in the lower cap dolostone successions are likely induced by changes in chemical compositions of the shelf seawater (see section 6.4 for details).

#### 6.4. A meltwater–seawater mixing model

With no evidence for a transition in diagenetic conditions or in marine carbonate mineralogies, the large negative Ca isotope excursion preserved in three widely separated Ediacaran cap dolostone sections was likely caused by a short-term but gradual change in composition of shelf seawater in which primary aragonite precipitated and then immediately dolomitized. The change in chemical compositions of the shelf seawater might have occurred due to varying addition of deglacial meltwater and runoff. Two aspects of deglaciation that are important for shelf marine conditions in this context are introduction of ice melt water and re-invigoration of continental weathering fluxes under warm and high atmospheric  $\text{CO}_2$  conditions (Hoffman et al., 1998), generating large volumes of runoff saturated with cations such as  $\text{Ca}^{2+}$  and  $\text{Mg}^{2+}$ . As mentioned above, we consider shelf seawater as the fluid in which the cap dolostone formed. The composition of this fluid is controlled by the relative proportion of freshwater influx from terrestrial meltwater and deglacial runoff mixing with original sea-

water (possibly a brine, Hoffman et al., 2017) in the aftermath of the Marinoan glaciation.

Negative  $\delta^{44}\text{Ca}$  excursions and generally low  $\delta^{44}\text{Ca}$  values in modern and ancient carbonates can be attributed to the influence of fresh water through a mechanism such as riverine input or submarine groundwater discharge, as freshwater generally has much lower  $\delta^{44}\text{Ca}$  values than contemporaneous seawater (Holmden et al., 2012a, 2012b; Shao et al., 2018). Therefore, it is possible that the negative Ca isotope excursion in the Marinoan cap dolostones may have been caused by addition of freshwater with relatively low  $\delta^{44}\text{Ca}$  values derived from ice melt and renewed continental runoff during deglaciation. Previous work has suggested the relatively long-term persistence of a freshwater lens or layer above alkaline (global) seawater on shallow marine shelves due to large influxes of (marine and meteoric derived) melt water during deglaciation, and in the aftermath of the Marinoan glaciation, which could have contributed to low  $\delta^{44}\text{Ca}$  values in cap carbonates (Shields, 2005; Yang et al., 2017). An input peak of the abundant calcium- and magnesium-bicarbonate, dissolved in meltwater from renewed chemical weathering under high atmospheric  $\text{CO}_2$  conditions just after ice sheet melting (Hoffman et al., 1998; Fabre and Berger, 2012), may have been incorporated in shallow seawater, resulting in the lowest  $\delta^{44}\text{Ca}$  signatures of the lower cap dolostones. The variation in  $\delta^{44}\text{Ca}$  values may have resulted from varying proportions of glacial meltwater and continental deglacial runoff rich in light Ca-isotope incorporated into shelf seawater. This freshwater influx scenario is also supported by  $^{87}\text{Sr}/^{86}\text{Sr}$  ratios in the three cap dolostone successions (Fig. 2). All of the sections in this study show a positive excursion in  $^{87}\text{Sr}/^{86}\text{Sr}$  ratios in the lower part of the cap dolostone, in step with the negative  $\delta^{44}\text{Ca}$  excursion. As more radiogenic  $^{87}\text{Sr}/^{86}\text{Sr}$  values are associated with fluids that have interacted with crustal material, especially freshly exposed, physically weathered minerals under glacial–interglacial cyclic conditions (Blum and Erel, 1995), the positive excursion in  $^{87}\text{Sr}/^{86}\text{Sr}$  in cap dolostones may have also resulted from the increased influence of meltwater and runoff (from freshly-exposed continental rocks) mixing into marine shelf waters in the immediate aftermath of the Marinoan glaciation. In this scenario, the deposition of the lowermost cap carbonate may have been influenced by meltwater from sea ice melt, at the onset of the deglaciation, and the peak of  $^{87}\text{Sr}/^{86}\text{Sr}$  and  $\delta^{44}\text{Ca}$  excursions would mark the maximum continental weathering input via terrestrial ice meltwater/runoff accompanying the deglaciation.

Based on the initial modeling results suggesting a fluid-buffered dolomitization condition for cap dolostone deposition (Fig. 5), a combined diagenetic and fluid mixing model can highlight the link between the Ca and Sr isotopic variations in the cap dolostone successions during freshwater–seawater fluid mixing (Fig. 6). In this model, we characterize a seawater end-member by high  $\delta^{44}\text{Ca}$  (1.5‰, slightly higher than the  $\delta^{44}\text{Ca}$  value of the most basal dolostones in this study, but lower than that of modern seawater) and low  $^{87}\text{Sr}/^{86}\text{Sr}$  (0.7070, Halverson et al., 2010) considering limited continental input into ice covered oceans during the ‘Snowball Earth’ period. The deglacial fresh water end-member (melt water and runoff) is assumed to have low  $\delta^{44}\text{Ca}$  (0.89‰, similar to the modern riverine value or continental crust value (e.g., Gussone et al., 2016) and high  $^{87}\text{Sr}/^{86}\text{Sr}$  (0.7150, similar to average upper continental crust value and higher than modern average riverine value) (e.g., Blum and Erel, 1995). Further, the primarily precipitated carbonate mineral is suggested as aragonite with low  $\delta^{44}\text{Ca}$  (0–0.3‰, controlled by contemporaneous seawater) and  $^{87}\text{Sr}/^{86}\text{Sr}$  (0.7070, Halverson et al., 2010), which is supported by ubiquitous aragonite precipitation during the Neoproterozoic (e.g., Hood and Wallace, 2018; Pruss et al., 2018).

Modeling results shown in Fig. 6A suggest that a mixing between freshwater and original seawater, in which approximately



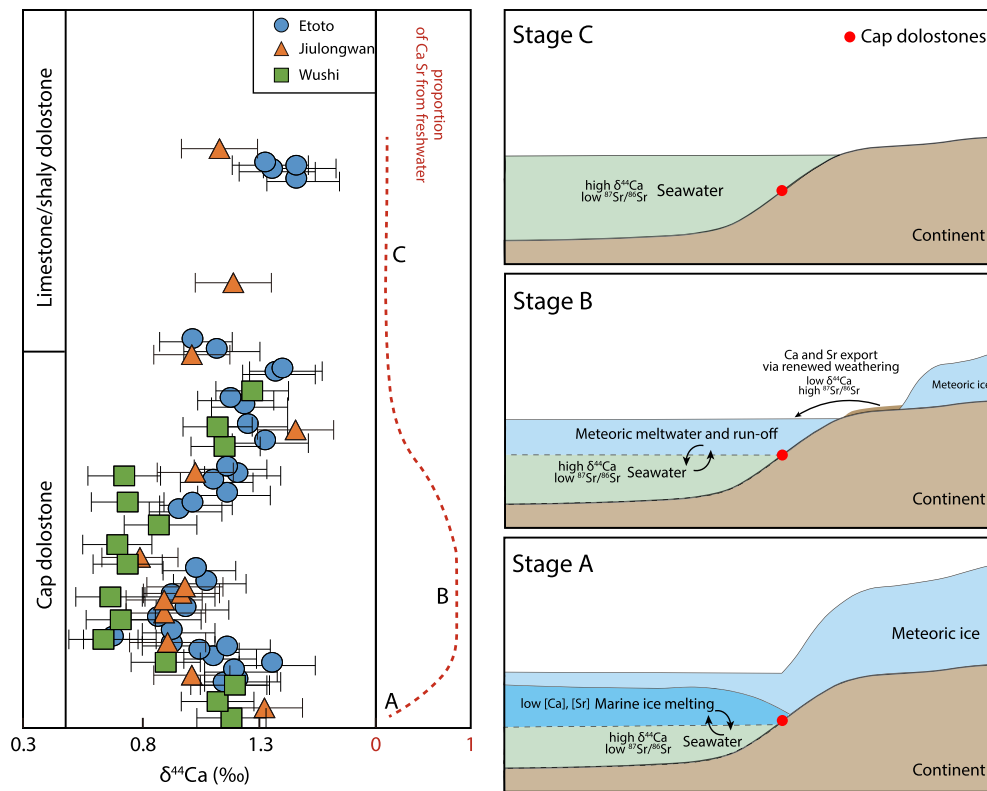


**Fig. 7.** Compilation of Ca isotope data from the cap dolostones in this study (Error bar for Ca isotopes is  $\pm 0.15$ , 2SD) and three-stage (A, B, C) schematic diagram for the cap dolostone formation. The systematic negative Ca isotope excursions are derived from the relative influence of varying dolomitizing fluids during and immediately following Marinoan deglaciation: (A) mixing of seawater (high  $\delta^{44}\text{Ca}$  and low  $^{87}\text{Sr}/^{86}\text{Sr}$ ) and melting marine ice (with little Ca and Sr); (B) mixing of seawater (high  $\delta^{44}\text{Ca}$  and low  $^{87}\text{Sr}/^{86}\text{Sr}$ ) and terrestrial meltwater/runoff (low  $\delta^{44}\text{Ca}$  and high  $^{87}\text{Sr}/^{86}\text{Sr}$ ); (C) seawater (high  $\delta^{44}\text{Ca}$  and low  $^{87}\text{Sr}/^{86}\text{Sr}$ ) as a dominant dolomitized fluid.

60%–80% of total Ca and Sr were derived from freshwater (terrestrial meltwater and deglacial runoff) and 20%–40% of total Ca and Sr were from shelf brine, could induce the peak of the Ca and Sr isotopic excursions in the lower cap dolostones. A compilation of Ca isotope data and the suggested freshwater–seawater mixing scenario for the dolomitizing fluid (i.e. freshwater–seawater mixture) are shown in Fig. 7. It should be noted that the  $\delta^{44}\text{Ca}$  values of the lowermost cap dolostones are higher than those of modern freshwater, which may have been a result of mixing between the original shelf seawater and early-stage melting sea ice (with only minor Ca, Sr concentrations in marine ice sheet) (Fig. 7, Stage A). Subsequent Ca isotope excursion as well as radiogenic Sr isotope excursion in the lower part of the cap dolostones is suggested to have resulted from a transition to mixing between the shelf seawater and a higher proportion of terrestrial meltwater and deglacial runoff (Fig. 7, Stage B).

The results of this simplified two end-member model can also help explain other geochemical records from cap dolostones. Although  $\delta^{18}\text{O}$  values of carbonate can be altered through interaction or exchange with non-marine fluids during burial diagenesis (e.g., possibly producing the extremely low  $\delta^{18}\text{O}$  of the Wushi section), the  $\delta^{18}\text{O}$  trends recorded in these cap dolostones, including negative anomalies in the Etoto section and the Jiulongwan sections (at the same time as the negative Ca excursion, Fig. 2), were possibly also driven by the addition of  $^{18}\text{O}$  depleted freshwater. Similarly, negative  $\delta^{13}\text{C}$  values of the cap dolostones have been attributed to an influx of deglacial continental runoff that had a much lower C isotopic composition than seawater during fluid-buffered dolomitization (e.g., Higgins and Schrag, 2003). In addition, negative  $\delta^{11}\text{B}$  excursions in the cap dolostones were suggested to indicate global ocean acidification (and high  $p\text{CO}_2$ ) in the aftermath of Marinoan glaciation (Kasemann et al., 2014; Ohnemüller et al., 2014). However, it is possible that these B iso-

topic excursions could also be explained by the influx of deglacial runoff (cf. Stewart et al., 2015) since freshwater pH ( $\sim 7$ ) is generally distinctly lower than seawater (pH  $> 8$ ) at the same (modern) atmospheric  $\text{CO}_2$  levels and  $\delta^{11}\text{B}$  signatures are different between seawater and freshwater sources. Additionally, cap dolostones generally have low Y/Ho ratios (e.g., Ling et al., 2013; this study), which could also be influenced by the addition of freshwater (cf. Zhao and Zheng, 2017).

#### 6.5. Implications for cap dolostone deposition in the aftermath of the Marinoan glaciation

Large negative Ca isotopic excursions in cap dolostones from three globally separated sections are suggested to have been caused by paleo-environmental conditions in the aftermath of the Marinoan glaciation. While Ca isotopic excursions could possibly be derived from fluctuations in the global marine Ca reservoir (over  $\sim 1$  Myr timescale), coupled Ca–Sr isotope excursions in the lower cap dolostone succession are more likely to have been caused by the mixing of deglacial ice meltwater and/or subsequent continental runoff into seawater (over a shorter timescale:  $10^4$  years, e.g., Crockford et al., 2016). Although marine synsedimentary dolomitization could have been widespread in Cryogenian seawater (e.g. Hood and Wallace, 2012), possibly caused by the high global marine Ca and Mg saturation linked to dissolution of volcanic materials (Gernon et al., 2016), our Ca–Sr data (negative  $\delta^{44}\text{Ca}$  and positive  $^{87}\text{Sr}/^{86}\text{Sr}$  excursions in the lower cap dolostones) support the suggestion that the mixing of deglacial meltwater/runoff and seawater in the aftermath of the Marinoan glaciation may also have promoted dolomitization through the increased import of  $\text{Ca}^{2+}$ ,  $\text{Mg}^{2+}$  and bicarbonate onto marine shelves.

While we cannot directly constrain atmospheric CO<sub>2</sub> levels during this time, the Ca–Sr isotope excursions found in this study indicate a high weathering flux into shelf seawater, which is consistent with relatively high atmospheric CO<sub>2</sub> concentrations (promoting high silicate weathering) during and immediately following Marinoan deglaciation. Under the ‘Snowball Earth’ hypothesis, and supported by triple-oxygen isotope data, the termination of the Marinoan glaciation is thought to have been characterized by dramatically high atmospheric CO<sub>2</sub> (10<sup>4</sup>–10<sup>5</sup> ppmv) (e.g., Hoffman et al., 1998; Bao et al., 2009). This extreme greenhouse climate has been proposed to significantly accelerate silicate weathering in the aftermath of glaciation, promoting the dissolution of mechanically eroded bedrock and liberating abundant cations and bicarbonate from newly exposed glacial landscapes (e.g., Fabre and Berger, 2012). The mixing of this runoff into shallow seawater is manifested in the low δ<sup>44</sup>Ca and high <sup>87</sup>Sr/<sup>86</sup>Sr values recorded in the lower cap dolostones. Therefore, it is likely that the formation of cap dolostones could have been promoted by a combination of an increased saturation state in the continental shelf surface seawater driven by intense chemical weathering, large amounts of runoff and high seawater temperatures in the immediate aftermath of the Marinoan glaciation (Hoffman et al., 2017).

## 7. Summary and conclusions

New high-resolution calcium isotopic records are reported for the cap dolostones from three widely-separated sections (South China, North China and Namibia) deposited in the immediate aftermath of the Neoproterozoic Marinoan glaciation. All these sections are characterized by a negative δ<sup>44</sup>Ca excursion on the order of 0.6‰ in the lower cap dolostones. This Ca isotopic anomaly is larger than those seen in the Phanerozoic records and cannot be interpreted as perturbation of the global oceanic Ca cycle using a time-dependent mass balance model given the relatively short duration of the cap dolostone (~10<sup>4</sup> year timescale). Together with low Sr concentrations and high <sup>87</sup>Sr/<sup>86</sup>Sr ratios in cap dolostones, the significant Ca isotopic anomaly is considered to have been a result of the dynamic mixing of deglacial freshwater (meltwater/runoff) and seawater, which may have also enhanced carbonate precipitation and synsedimentary dolomitization to form the cap dolostone. The low δ<sup>44</sup>Ca and high <sup>87</sup>Sr/<sup>86</sup>Sr characteristics of the cap dolostones are suggested to have been derived from the combined effects of intense continental weathering and large volumes of meltwater/runoff in the aftermath of Marinoan glaciation.

## Acknowledgements

We thank Dr. Dan Asael for assistance with the lab work; Dr. Noah J. Planavsky and Ming-Yu Zhao for useful discussion and Emily Stewart for collecting samples. We gratefully acknowledge the constructive comments by Editor Prof. Derek Vance and three anonymous reviewers. This study was funded by the Strategic Priority Research Program (B) of the Chinese Academy of Sciences (CAS) (XDB26000000) and the National Natural Science Foundation of China (NSFC) program (41661134048, 41672026, 41872002). Guang-Yi Wei is also funded by a state scholarship grant from China Scholarship Council (CSC) and the program A for Outstanding PhD. Candidate of Nanjing University (No. 201802A020). A.v.S. Hood acknowledges a NASA Astrobiology Postdoctoral Fellowship and the University of Melbourne Puzey Fellowship.

## Appendix A. Supplementary material

Supplementary material related to this article can be found online at <https://doi.org/10.1016/j.epsl.2019.01.024>.

## References

- Ahm, A.-S.C., Bjerrum, C.J., Blättler, C.L., Swart, P.K., Higgins, J.A., 2018. Quantifying early marine diagenesis in shallow-water carbonate sediments. *Geochim. Cosmochim. Acta* 236, 140–159.
- Banner, J.L., 1995. Application of the trace element and isotope geochemistry of strontium to studies of carbonate diagenesis. *Sedimentology* 42 (5), 805–824.
- Bao, H., Fairchild, I.J., Wynn, P.M., Spötl, C., 2009. Stretching the envelope of past surface environments: Neoproterozoic glacial lakes from Svalbard. *Science* 323, 119–122.
- Blättler, C.L., Jenkyns, H.C., Reynard, L.M., Henderson, G.M., 2011. Significant increases in global weathering during Oceanic Anoxic Events 1a and 2 indicated by calcium isotopes. *Earth Planet. Sci. Lett.* 309 (1), 77–88.
- Blum, J.D., Erel, Y., 1995. A silicate weathering mechanism linking increases in marine <sup>87</sup>Sr/<sup>86</sup>Sr with global glaciation. *Nature* 373 (6513), 415–418.
- Bristow, T.F., Bonifacie, M., Derkowski, A., Eiler, J.M., Grotzinger, J.P., 2011. A hydrothermal origin for isotopically anomalous cap dolostone cements from south China. *Nature* 474 (7349), 68–71.
- Burns, S.J., McKenzie, J.A., Vasconcelos, C., 2000. Dolomite formation and biogeochemical cycle in the Phanerozoic. *Sedimentology* 47, 49–61.
- Condon, D., Zhu, M., Bowring, S., Wang, W., Yang, A., Jin, Y., 2005. U–Pb ages from the Neoproterozoic Doushantuo Formation, China. *Science* 308 (5718), 95–98.
- Crockford, P.W., Cowie, B.R., Johnston, D.T., Hoffman, P.F., Sugiyama, I., Pellerin, A., Bui, T.H., Hayles, J., Halverson, G.P., Macdonald, F.A., Wing, B.A., 2016. Triple oxygen and multiple sulfur isotope constraints on the evolution of the post-Marinoan sulfur cycle. *Earth Planet. Sci. Lett.* 435, 74–83.
- Fabre, S., Berger, G., 2012. How tillite weathering during the Snowball Earth aftermath induced cap carbonate deposition. *Geology* 40 (11), 1027–1030.
- Fabre, S., Berger, G., Chavagnac, V., Besson, P., 2013. Origin of cap carbonates: an experimental approach. *Palaeogeogr. Palaeoclimatol. Palaeoecol.* 392, 524–533.
- Fantle, M.S., DePaolo, D.J., 2007. Ca isotopes in carbonate sediment and pore fluid from ODP Site 807A: the Ca<sup>2+</sup>(aq)–calcite equilibrium fractionation factor and calcite recrystallization rates in Pleistocene sediments. *Geochim. Cosmochim. Acta* 71 (10), 2524–2546.
- Fantle, M.S., Tipper, E.T., 2014. Calcium isotopes in the global biogeochemical Ca cycle: implications for development of a Ca isotope proxy. *Earth-Sci. Rev.* 129, 148–177.
- Font, E., Nédélec, A., Trindade, R., Macouin, M., Charriere, A., 2006. Chemostratigraphy of the Neoproterozoic Mirassol d’Oeste cap dolostones (Mato Grosso, Brazil): an alternative model for Marinoan cap dolostone formation. *Earth Planet. Sci. Lett.* 250 (1–2), 89–103.
- Font, E., Nédélec, A., Trindade, R., Moreau, C., 2010. Fast or slow melting of the Marinoan Snowball Earth? The cap dolostone record. *Palaeogeogr. Palaeoclimatol. Palaeoecol.* 295 (1–2), 215–225.
- Gammon, P.R., 2012. An organodiagenetic model for Marinoan-age cap carbonates. *Sediment. Geol.* 243–244, 17–32.
- Gernon, T.M., Hincks, T.K., Tyrrell, T., Rohling, E.J., Palmer, F.A.R., 2016. Snowball Earth ocean chemistry driven by extensive ridge volcanism during Rodinia breakup. *Nat. Geosci.* 9 (3), 242–248.
- Gussone, N., Schmitt, A.D., Heuser, A., Wombacher, F., Dietzel, M., Tipper, E., Schiller, M., 2016. Calcium Stable Isotope Geochemistry. Springer.
- Halverson, G.P., Wade, B.P., Hurtgen, M.T., Barovich, K.M., 2010. Neoproterozoic chemostratigraphy. *Precambrian Res.* 182 (4), 337–350.
- Higgins, J.A., Blättler, C.L., Lundstrom, E.A., Santiago-Ramos, D.P., Akhtar, A.A., Crüger Ahm, A.S., Bialik, O., Holmden, C., Bradbury, H., Murray, S.T., Swart, P.K., 2018. Mineralogy, early marine diagenesis, and the chemistry of shallow-water carbonate sediments. *Geochim. Cosmochim. Acta* 220, 512–534.
- Higgins, J.A., Schrag, D.P., 2003. Aftermath of a Snowball Earth. *Geochem. Geophys. Geosyst.* 4 (3), 1028.
- Hoffman, P.F., 2011. Strange bedfellows: glacial diamicrite and cap carbonate from the Marinoan (635 Ma) glaciation in Namibia. *Sedimentology* 58 (1), 57–119.
- Hoffman, P.F., Abbot, D.S., Ashkenazy, Y., Benn, D.I., Brocks, J.J., Cohen, P.A., Cox, G.M., Creveling, J.R., Donnadieu, Y., Erwin, D.H., Fairchild, I.J., Ferreira, D., Goodman, J.C., Halverson, G.P., Jansen, M.F., Le Hir, G., Love, G.D., Macdonald, F.A., Maloof, A.C., Partin, C.A., Ramstein, G., Rose, B.E.J., Rose, C.V., Sadler, P.M., Tziperman, E., Voigt, A., Warren, S.G., 2017. Snowball Earth climate dynamics and Cryogenian geology–geobiology. *Sci. Adv.* 3 (11).
- Hoffman, P.F., Kaufman, A.J., Halverson, G.P., Schrag, D.P., 1998. A Neoproterozoic Snowball Earth. *Science* 281, 1342–1346.
- Hoffman, P.F., Halverson, G.P., Domack, E.W., Husson, J.M., Higgins, J.A., Schrag, D.P., 2007. Are basal Ediacaran (635 Ma) post-glacial “cap dolostones” diachronous? *Earth Planet. Sci. Lett.* 258 (1), 114–131.
- Hoffman, P.F., Li, Z.X., 2009. A palaeogeographic context for Neoproterozoic glaciation. *Palaeogeogr. Palaeoclimatol. Palaeoecol.* 277 (3), 158–172.
- Holmden, C., Panchuk, K., Finney, S.C., 2012a. Tightly coupled records of Ca and C isotope changes during the Hirnantian glaciation event in an epeiric sea setting. *Geochim. Cosmochim. Acta* 98, 94–106.
- Holmden, C., Papanastassiou, D.A., Blanchon, P., Evans, S., 2012b. δ<sup>44</sup>/40Ca variability in shallow water carbonates and the impact of submarine groundwater discharge on Ca-cycling in marine environments. *Geochim. Cosmochim. Acta* 83, 179–194.

- Hood, A.v.S., Wallace, M.W., 2012. Synsedimentary diagenesis in a Cryogenian reef complex: ubiquitous marine dolomite precipitation. *Sediment. Geol.* 255–256, 56–71.
- Hood, A.v.S., Wallace, M.W., 2015. Extreme ocean anoxia during the Late Cryogenian recorded in reefal carbonates of Southern Australia. *Precambrian Res.* 261, 96–111.
- Hood, A.v.S., Wallace, M.W., 2018. Neoproterozoic marine carbonates and their paleoceanographic significance. *Glob. Planet. Change* 160, 28–45.
- Jiang, G., Kennedy, M.J., Christie-Blick, N., 2003. Stable isotopic evidence for methane seeps in Neoproterozoic postglacial cap carbonates. *Nature* 426, 822–826.
- Jost, A.B., Bachan, A., van de Schootbrugge, B., Brown, S.T., DePaolo, D.J., Payne, J.L., 2017. Additive effects of acidification and mineralogy on calcium isotopes in Triassic/Jurassic boundary limestones. *Geochim. Geophys. Geosyst.* 18. <https://doi.org/10.1002/2016GC006724>.
- Kasemann, S.A., von Strandmann, P.A.P., Prave, A.R., Fallick, A.E., Elliott, T., Hoffmann, K.H., 2014. Continental weathering following a Cryogenian glaciation: evidence from calcium and magnesium isotopes. *Earth Planet. Sci. Lett.* 396, 66–77.
- Kennedy, M.J., Christie-Blick, N., 2011. Condensation origin for Neoproterozoic cap carbonates during deglaciation. *Geology* 39 (4), 319–322.
- Land, L.S., 1973. Holocene meteoric dolomitization of Pleistocene limestones, North Jamaica. *Sedimentology* 20, 411–424.
- Lau, K.V., Maher, K., Brown, S.T., Jost, A.B., Altnner, D., DePaolo, D.J., Eisenhauer, A., Kelley, B.M., Lehrmann, D.J., Paytan, A., Silva-Tamayo, J.C., Yu, M., Payne, J.L., 2017. The influence of seawater carbonate chemistry, mineralogy, and diagenesis on calcium isotope variations in Lower–Middle Triassic carbonate rocks. *Chem. Geol.* 471, 13–37.
- Li, D., Shields-Zhou, G.A., Ling, H.-F., Thirlwall, M., 2011. Dissolution methods for strontium isotope stratigraphy: guidelines for the use of bulk carbonate and phosphorite rocks. *Chem. Geol.* 290 (3–4), 133–144.
- Li, Z.X., Bogdanova, S.V., Collins, A.S., Davidson, A., De Waele, B., Ernst, R.E., Fitzsimons, I.C.W., Fuck, R.A., Gladkochub, D.P., Jacobs, J., Karlstrom, K.E., Lu, S., Natapov, L.M., Pease, V., Pisarevsky, S.A., Thrane, K., Vernikovsky, V., 2008. Assembly, configuration, and break-up history of Rodinia: a synthesis. *Precambrian Res.* 160 (1–2), 179–210.
- Ling, H.-F., Chen, X., Li, D., Wang, D., Shields-Zhou, G.A., Zhu, M., 2013. Cerium anomaly variations in Ediacaran–earliest Cambrian carbonates from the Yangtze Gorges area, South China: implications for oxygenation of coeval shallow seawater. *Precambrian Res.* 225, 110–127.
- Liu, C., Wang, Z., Raub, T.D., Macdonald, F.A., Evans, D.A.D., 2014. Neoproterozoic cap-dolostone deposition in stratified glacial meltwater plume. *Earth Planet. Sci. Lett.* 404, 22–32.
- Ohnemüller, F., Prave, A.R., Fallick, A.E., Kasemann, S.A., 2014. Ocean acidification in the aftermath of the Marinoan glaciation. *Geology* 42 (12), 1103–1106.
- Payne, J.L., Turchyn, A.V., Paytan, A., DePaolo, D.J., Lehrmann, D.J., Yu, M., Wei, J., 2010. Calcium isotope constraints on the end-Permian mass extinction. *Proc. Natl. Acad. Sci. USA* 107 (19), 8543–8548.
- Pruss, S.B., Blättler, C.L., Macdonald, F.A., Higgins, J.A., 2018. Calcium isotope evidence that the earliest metazoan biomineralizers formed aragonite shells. *Geology* 46 (9), 763–766.
- Ridgwell, A., Kennedy, M.J., Caldeira, K., 2003. Carbonate deposition, climate stability, and Neoproterozoic ice ages. *Science* 302, 859–862.
- Rose, C.V., Maloof, A.C., 2010. Testing models for post-glacial 'cap dolostone' deposition: Nuccaleena Formation, South Australia. *Earth Planet. Sci. Lett.* 296 (3–4), 165–180.
- Sánchez-Román, M., McKenzie, J.A., Wagener, A.D.L.R., Romanek, C.S., Sánchez-Navas, A., Vasconcelos, C., 2011. Experimentally determined biomediated Sr partition coefficient for dolomite: significance and implication for natural dolomite. *Geochim. Cosmochim. Acta* 75 (3), 887–904.
- Sawaki, Y., Ohno, T., Tahata, M., Komiya, T., Hirata, T., Maruyama, S., Windley, B.F., Han, J., Shu, D., Li, Y., 2010. The Ediacaran radiogenic Sr isotope excursion in the Doushantuo Formation in the Three Gorges area, South China. *Precambrian Res.* 176 (1–4), 46–64.
- Shao, Y.X., Farkas, J., Holmden, C., Mosley, L., Kell-Duivesteyn, I., Izzo, C., Reis-Santos, P., Tyler, J., Torber, P., Fryda, J., Taylor, H., Haynes, D., Tibby, J., Gillanders, B.M., 2018. Calcium and strontium isotope systematics in the lagoon-estuarine environments of South Australia: implications for water source mixing, carbonate fluxes and fish migration. *Geochim. Cosmochim. Acta* 239, 90–108.
- Shields, G.A., 2005. Neoproterozoic cap carbonates: a critical appraisal of existing models and the plume world hypothesis. *Terra Nova* 17 (4), 299–310.
- Sial, A.N., Gaucher, C., da Silva Filho, M.A., Ferreira, V.P., Pimentel, M.M., Lacerda, L.D., Silva Filho, E.V., Cezario, W., 2010. C-, Sr-isotope and Hg chemostratigraphy of Neoproterozoic cap carbonates of the Sergipano Belt, Northeastern Brazil. *Precambrian Res.* 182 (4), 351–372.
- Silva-Tamayo, J.C., Nägler, T.F., Sial, A.N., Nogueira, A., Kyser, K., Riccomini, C., James, N.P., Narbonne, G.M., Villa, I.M., 2010. Global perturbation of the marine Ca isotopic composition in the aftermath of the Marinoan global glaciation. *Precambrian Res.* 182 (4), 373–381.
- Stewart, J.A., Gutjahr, M., Pearce, F., Swart, P.K., Foster, G.L., 2015. Boron during meteoric diagenesis and its potential implications for Marinoan Snowball Earth  $\delta^{11}\text{B}$ -pH excursions. *Geology* 43 (7), 627–630.
- Swart, P.K., Ruiz, J., Holmes, C.W., 1987. Use of strontium isotopes to constrain the timing and mode of dolomitization of upper Cenozoic sediments in a core from San Salvador, Bahamas. *Geology* 15, 262–265.
- Tang, J., Dietzel, M., Böhm, F., Köhler, S.J., Eisenhauer, A., 2008.  $\text{Sr}^{2+}/\text{Ca}^{2+}$  and  $^{44}\text{Ca}/^{40}\text{Ca}$  fractionation during inorganic calcite formation: II. Ca isotopes. *Geochim. Cosmochim. Acta* 72 (15), 3733–3745.
- Wei, G.-Y., Planavsky, N.J., Tarhan, L.G., Chen, X., Wei, W., Li, D., Ling, H.-F., 2018. Marine redox fluctuation as a potential trigger for the Cambrian explosion. *Geology* 46 (7), 587–590.
- Wen, B., Evans, D.A., Li, Y.X., Wang, Z., Liu, C., 2015. Newly discovered Neoproterozoic diamicrite and cap carbonate (DCC) couplet in Tarim Craton, NW China: stratigraphy, geochemistry, and paleoenvironment. *Precambrian Res.* 271, 278–294.
- Yang, J., Jansen, M.F., Macdonald, F.A., Abbot, D.S., 2017. Persistence of a freshwater surface ocean after a Snowball Earth. *Geology* 45 (7), 615–618.
- Yoshioka, H., Asahara, Y., Tojo, B., Kawakami, S.I., 2003. Systematic variations in C, O, and Sr isotopes and elemental concentrations in Neoproterozoic carbonates in Namibia: implications for a glacial to interglacial transition. *Precambrian Res.* 124 (1), 69–85.
- Zhao, M.-Y., Zheng, Y.-F., 2017. A geochemical framework for retrieving the linked depositional and diagenetic histories of marine carbonates. *Earth Planet. Sci. Lett.* 460, 213–221.